TECHNICAL REPORT No. 38

THE RESPONSE OF THE ECMWF GLOBAL MODEL TO THE EL-NINO ANOMALY IN EXTENDED RANGE PREDICTION EXPERIMENTS

by

Ulrich Cubasch

September 1983

C O N T E N T S

Abstract

Numerical experiments have been carried out, using a low resolution version of the ECMWF general circulation model, to investigate the response of the atmosphere to a positive and negative sea surface temperature anomaly in the tropical Pacific during a 150 day integration period. The response in the tropical Pacific seems to be strongly correlated with the anomaly and resembles the one obtained by Gill (1980) using a shallow water equation model. The SST anomalies cause a pressure perturbation in the tropics similar to the observed "Southern Oscillation". A major warming, however, does not only occur in the region with the largest precipitation increase, but also in the area with sinking motion in the subtropics. The response in the mid-latitudes compares well with observed correlation pattern, but proves to be independent of the sign of the anomaly and is therefore difficult to reproduce using linear theories. Superimposed on the mean response are long period fluctuations whose amplitude reaches about 75% of the mean response. These fluctuations can also be found in the tropical precipitation deviation and might be caused by large scale convective cells similar to those observed and discussed by Madden and Julian (1971,1972).

1. INTRODUCTION

At a conference in Stockholm (August 1981) the Working Group on Numerical Experimentation (WGNE), in cooperation with the WMO, suggested a series of numerical experiments to investigate the impact of the El-Nino sea-surface temperature anomaly on the general circulation of the atmosphere.

This anomaly can be found at irregular intervals in the tropical Pacific between Indonesia and South America. A detailed desciption of its build up, maintenance and decay can be found in Rasmusson and Carpenter (1982). Their published anomaly for the month of January, when it is in its mature stage, has been used for all subsequent experiments (Fig. 1).

Bjerknes (1966,1969) pointed out in a synoptic study that the El-Nino anomaly appears not only to influence the tropical belt, but also (via an intensification of the Hadley cell) lead to changes in the mid-latitude climate. Namias (1969) went even further and tried to find a connection between the El-Nino phenomenon and anomalous seasons over North America.

The enthusiasm displayed in these observational studies stimulated a number of numerical experiments which tried to investigate the impact of SST anomalies on the general circulation (Rowntree, 1972, Houghton et al, 1974, Chervin et al, 1976, Kutzbach et al, 1977, Huang, 1978). These experiments remained generally inconclusive - partly because the short time series involved did not allow a meaningful evaluation and partly because it was not quite clear which mechanism governed the interaction between the SST-anomaly and atmosphere. It emerged, however, from these experiments that a heating in the tropics triggered off a better developed wavetrain than a heat source in mid-latitudes.

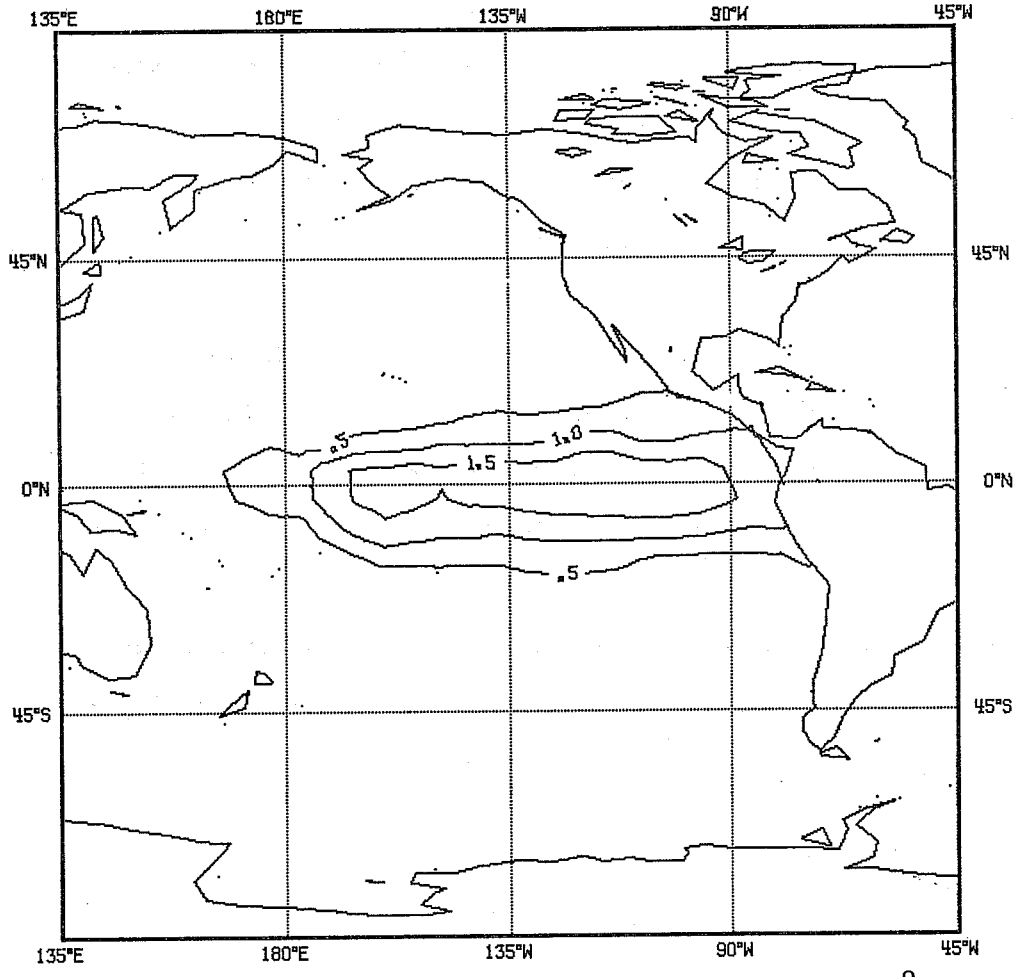

Fig. 1 The El-Nino sea surface temperature anomaly (units: ^{o}C).

A number of theoretical studies have also been carried out. Webster (1981) used a simple model to explain how the response varied with the latitude of the heating. At the same time Hoskins and Karoly (1981) used a linear model to simulate a Rossby wave train which was triggered off by a heat source. This wavetrain spreads from the heating region over the hemisphere and supports the ideas of Namias (1969) who suggested that the tropics interact with mid-latitudes by long, standing Rossby waves.

Simmons (1982) found similar wavetrains using a linear model, but showed that in a simple barotropic model the wavetrain can be strongly dependent on the location of the anomaly and on the planetary-wave structure of the basic state of the atmosphere. This has been further studied by Simmons et al (1983).

The recent successes of these theoretical studies encouraged the WGNE to suggest to a number of meteorological research institutions that they verify these results with general circulation models.

Two ways of doing these experiments were proposed:

(a) runs with and without the SST anomaly would be performed for "perpetual" January extending for more than 200 days;

(b) a control run would be made for the entire annual cycle over several years. An ensemble of anomaly runs would be made for the period December-January.

The first results of these experiments were presented at the "WGNE Workshop on SST Sensitivity Experiments" in Princeton, N.J., USA, 1982. Amongst the papers presented there are two which will be considered here; one by Blackmon et al (1982), which describes experiments following proposal (a) and the one

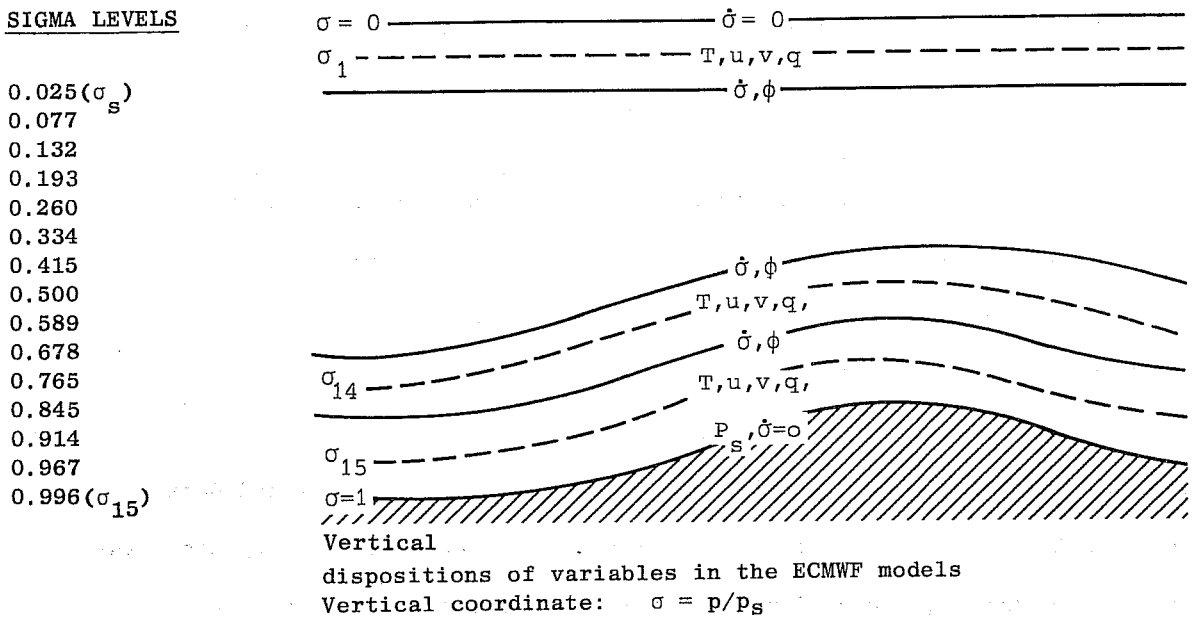

Vertical dispositions of variables in the ECMWF models
Vertical coordinate: $\sigma = p/p_s$

Independent variables	λ, φ, ϕ, t
Dependent variables	T, u, v, q, p_s
Grid	Gaussian, resolution : T21 max. resolved zonal wave nr. 21.
	non-uniform spacing of vertical levels.
Finite difference scheme	Second order accuracy.
Time-integration	Leapfrog, semi-implicit (Δt: T21-2400 sec)
Horizontal diffusion	Linear, fourth order (diffusion coefficient = T21-2.10^{15})
Earth surface	Albedo, roughness, soil moisture, snow and ice specified geographically. Albedo, soil moisture and snow time dependent.
Orography	Averaged from high resolution data set.
Vertical boundary conditions	$\dot{\sigma} = 0$ at $p = p_s$ and $p = 0$.
Physical parameterisation	(i) Boundary eddy fluxes dependent on roughness length and local stability (Monin Obukov)
	(ii) Free-atmosphere turbulent fluxes dependent on mixing length and Richardson number
	(iii) Kuo convection scheme
	(iv) Full interaction between radiation and clouds
	(v) Full hydrological cycle
	(vi) Computed land temperature, no diurnal cycle
	(vii) Climatological sea-surface temperature adjusted every 4th day.

Fig. 2 Characteristics of the ECMWF spectral model

by Shukla et al (1982), which deals with experiments made under proposal (b). In this report their findings will be discussed and compared with the ECMWF results.

The ECMWF experiment followed proposal (b). A first analysis, however, revealed large fluctuations in the response pattern. It was therefore decided to extend the integration period for the experiment to the period November to March, that is 150 days.

The experiments have been carried out starting from model generated data. These initial data where derived from a 10 year integration and represent the November of the first and of the ninth year of this long forecast. For historical reasons, most of the results refer to the simulation starting in November of the ninth year. The results of the run starting from the November of the first year are only used to support the findings of this integration.

2. THE MODEL EXPERIMENTS

2.1 The model

The model used in the experiments was a low resolution version of ECMWF's first spectral model (Baede et al, 1979), using the comprehensive operational parameterisation package for the simulation of the physical aspects (Tiedtke et al, 1978). It has 15 levels in the vertical on σ surfaces and resolves up to total wavenumber 21. Diabatic processes, which include the parametrisation of radiation, large scale condensation, turbulent vertical diffusion and cumulus convection, were calculated on a Gaussian grid with a spacing of about 5.6° of latitude.

The solar angle was adjusted every 12 hours to its climatological value but there was no diurnal cycle; the climatological soil moisture content, the sea-surface and deep soil temperature were modified every fourth day (for more details see Fig. 2).

This model has been integrated over a 10 year period. A detailed description of its performance can be found in Rilat and Thepaut (1982) and Volmer et al, (1983): the model appears to simulate the earth's atmosphere reasonably well, although its variability is less than observed. It is not yet clear whether this is a consequence of the boundary conditions, an effect of the low resolution or a deficiency of the model itself. Lau (1981) and Manabe and Hahn (1981) found a similar problem in their integration over 15 years with the GFDL model.

2.2 The experiment

The 10 year integration was restarted in November of the 9th year and integrated for 150 days. The only difference between the original and the restarted run was the altered sea-surface temperature, which now included the El-Nino SST anomaly in the Pacific.

This report will concentrate on the two main experiments:

a) 2* the El-Nino anomaly

b) -2* the El-Nino anomaly

The anomaly has been multiplied by a factor of 2 to enhance its effect on the circulation. The earlier shorter integrations showed that by only introducing the normal anomaly, the response pattern in mid-latitudes was fairly disorganized; the double anomaly produced reasonable looking wavetrains. Blackmon et al (1982) had to introduce the same factor in their model integrations in order to produce a well defined anomalous rainfall pattern in the anomaly region.

During the winter 1982/83 a strong anomaly (more than twice as high as the one described by Rasmusson and Carpenter (1982)) has been observed (CAC1, 1982) and this allows us to compare this recent El-Nino event directly with our model simulation.

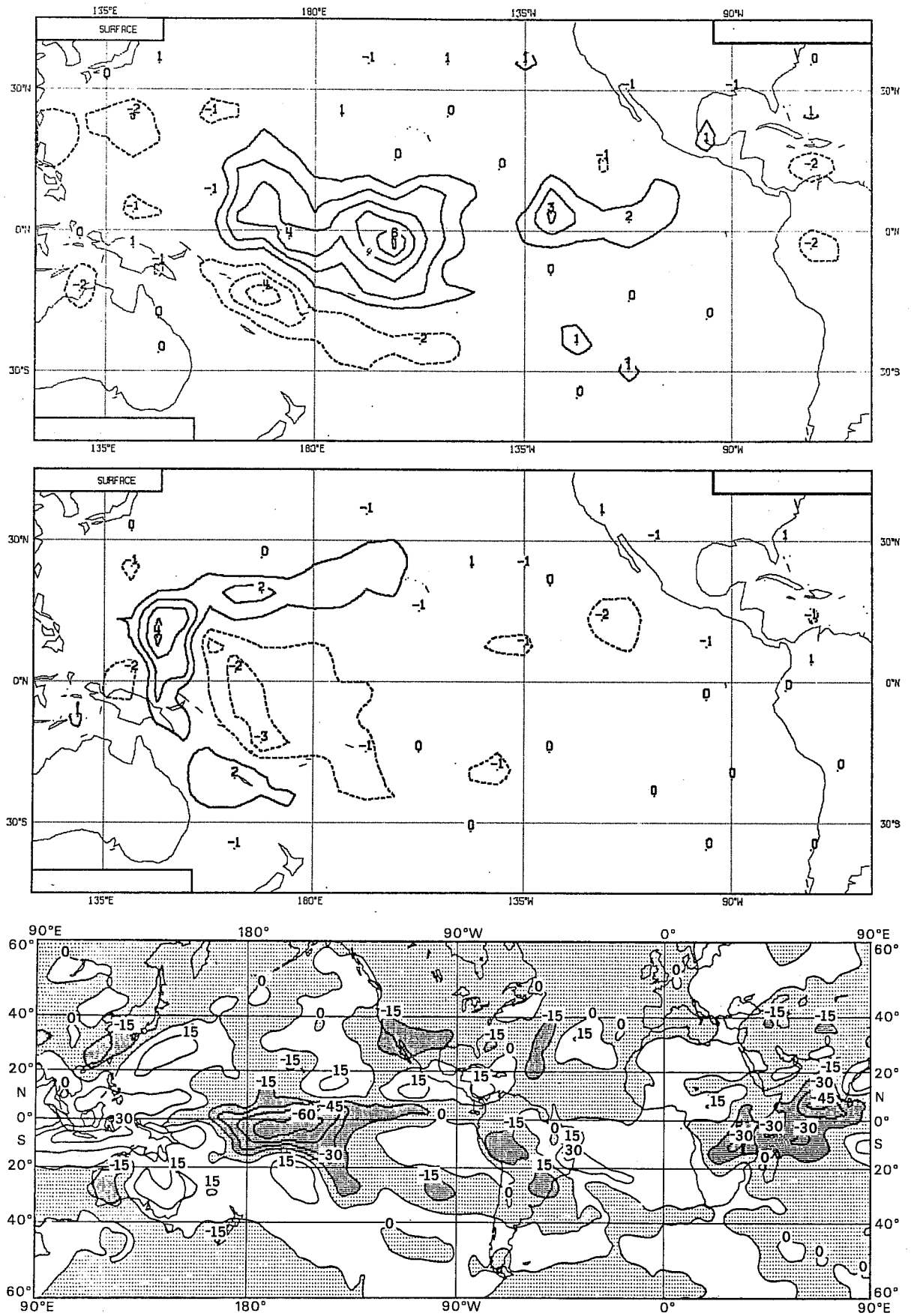

Fig. 3 The difference in the precipitation between anomaly runs and the control run. Top: positive anomaly, middle: negative anomaly, bottom: anomaly of outgoing longwave radiation as observed during November 1982. (units: precipitation,mm/day; radiation, W/m^2).

3. EVALUATION

After a preliminary assessment of the results of these experiments, it appeared to be necessary to make a distinction between the tropics and the mid-latitudes and to discuss them separately. Charts prepared by van Loon and Rogers (1981), Wallace and Gutzler (1981), van Loon et al, (1982) and maps made available by the CAC 1-3(1982/83) have been related to the model results and will be referred to in this study as observations.

3.1 Tropical response

3.1.1 The precipitation

An increase of the surface temperature is expected to destabilize the air and will lead under moist adiabatic unstable conditions (as can be found all over the tropical Pacific region) to an enhanced development of cumulus convection.

A change in cumulus convection can be diagnosed by an increased rainfall over the anomaly region for the positive anomaly and and decrease of precipitation for the negative anomaly (Fig. 3). West of the anomaly region one finds a negative (positive) precipitation deviation from the standard run for the positive (negative) anomaly; this indicates that the rainfall has not only been increased (decreased) by the anomaly, but also displaced from west of the anomaly region to the western part of the anomaly.

The fact that the rainfall has altered particularly over the western part of the anomaly can be explained by the climatological temperature distribution in the tropical Pacific. The eastern part of the tropical Pacific is colder than the western part. Due to the nonlinear dependence of the saturation of vapour pressure on the temperature, the amount of available water vapor is larger in the warmer western Pacific (Bjerknes, 1969).

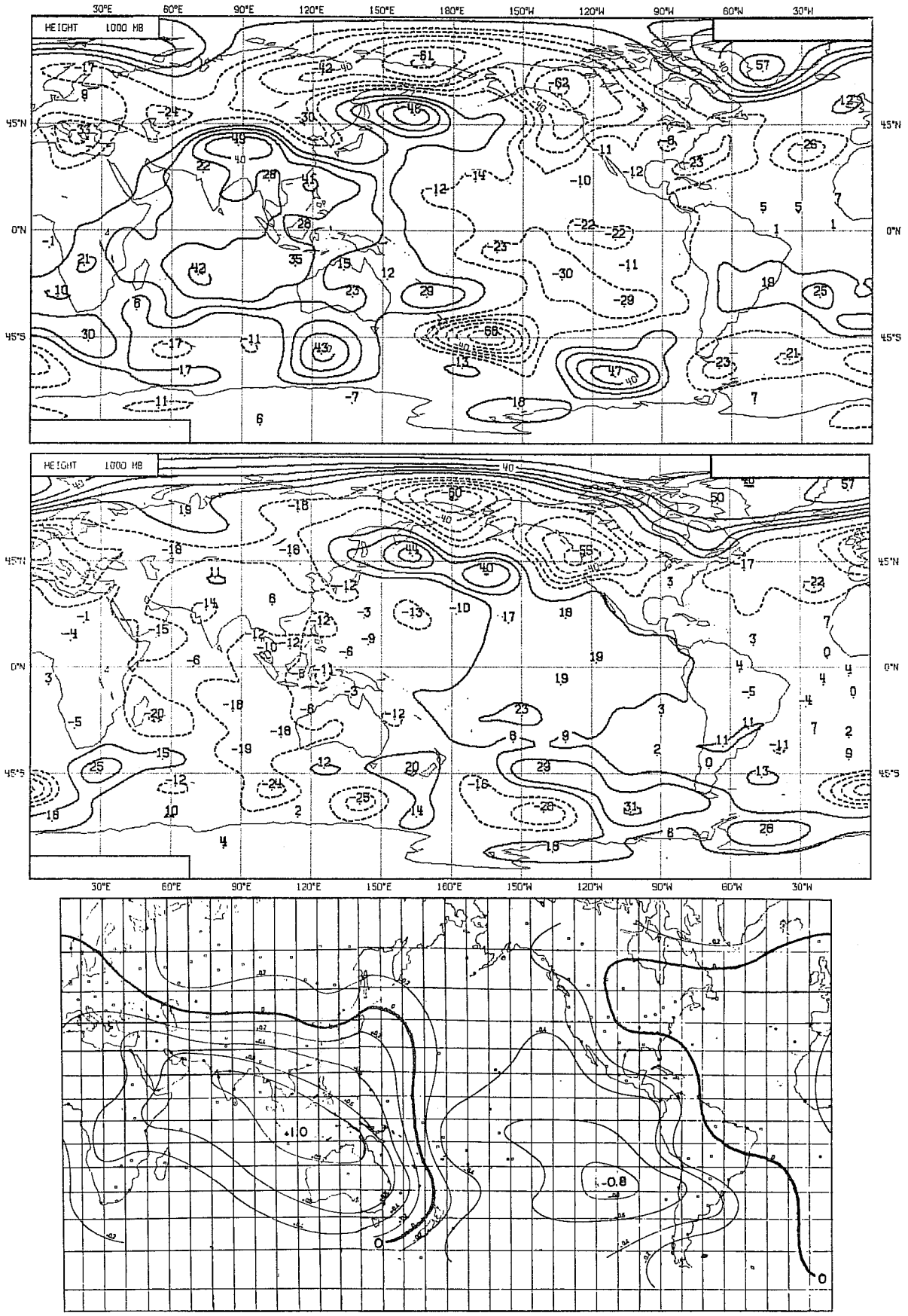

Fig. 4 The 1000 mb height field difference between anomaly runs and control experiment. Top: positive anomaly, middle: negative anomaly, bottom: Walkers Southern Oscillation correlation pattern; taken from Berlage, 1957. (contouring interval of heights fields: 10 m).

Note that a secondary, but smaller convection extremum has developed east of the first one.

It is worth trying to verify this model result by comparing it with the winter 1982/83. Rainfall, and particularly rainfall-anomalies, are difficult to analyse over oceanic regions because they are only measured by a small number of island stations. Therefore the usual way of assessing precipitation is to examine the outgoing longwave radiation derived from satellite observations (CAC1, 1982). Clouds absorb and emit infrared radiation like a black body. Therefore the amount of the radiation emitted is a function of the temperature of the cloud top. The higher the cloud top (i.e. the larger the cloud) the lower is the emission and probably the larger the precipitation.

Satellite pictures of the El-Nino region have been made available by the CAC 1-3 (1982/83). The area of the largest precipitation increase agrees well with the observed maximum in the cloudcover deviation for November 1982. The observations for the following month show an eastward drift of the maximum cloud cover which was not simulated by the model. This eastward shift was connected with an eastward drift of the temperature anomaly, perhaps caused by the anomalous wind field (Gill, 1983, pers.com.). It seems therefore that over a timescale of several months, the dynamic ocean atmosphere interaction is already important and ignoring it can lead to detectable deviations in a model simulation.

3.1.2 The height field

The pressure over the warm anomaly is decreased in the lower layers (Fig. 4) and raised in the higher levels. The negative anomaly produces the reverse effect.

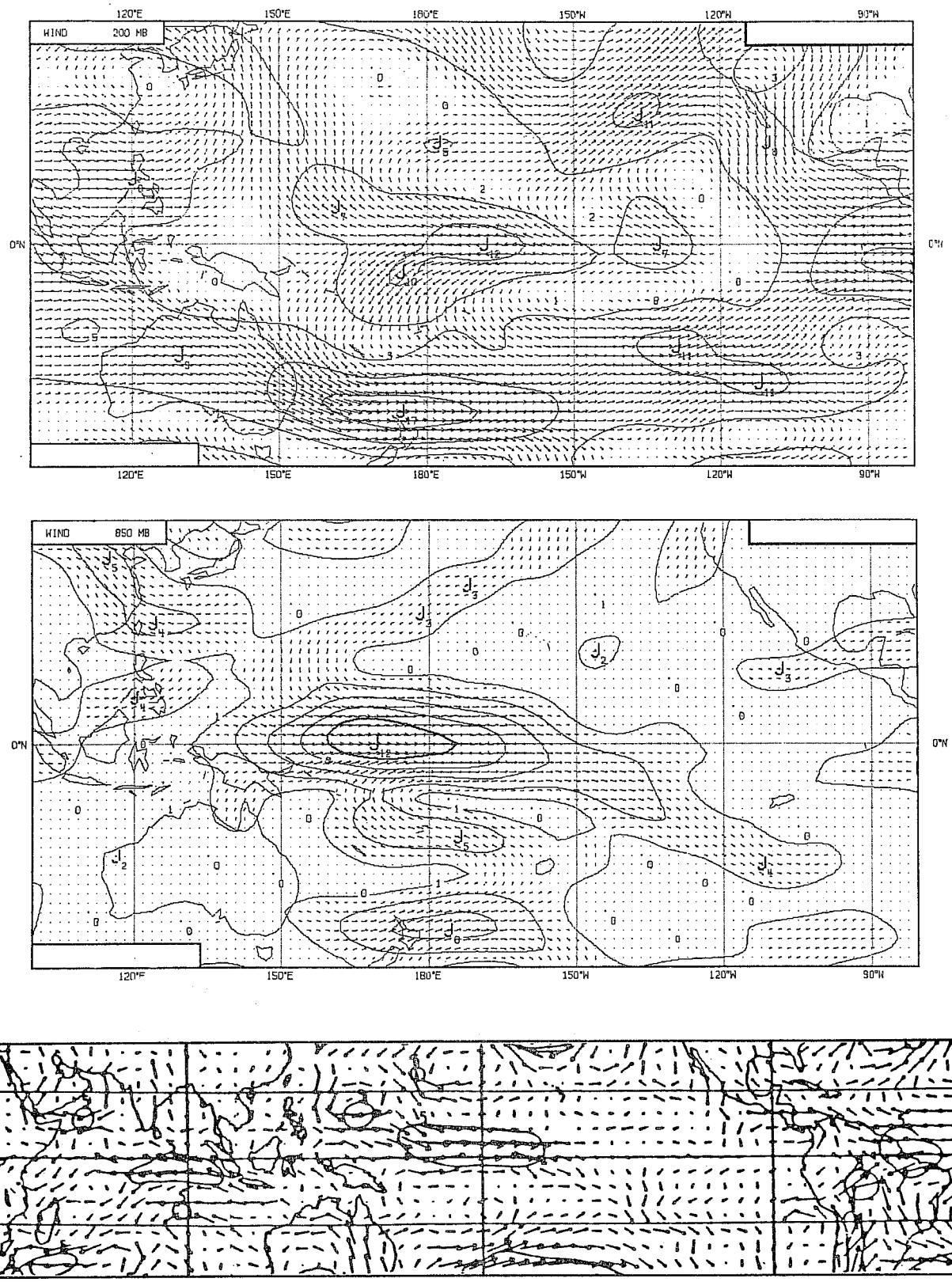

Fig. 5 The difference in the windfield of the run with the positive anomaly to the control run. Top: 200 mb height, middle: 850 mb, bottom: as observed during October 1982 in 850 mb (CAC 1).

Both anomalies excite a mean height response in the tropics resembling the pattern of the "Southern Oscillation" (Berlage, 1957). The axis of this oscillation is situated at around 165°E with the amplitude about 50 m for the positive anomaly and about 20 m for the negative one. Since such an oscillation was not found in the the 10 year integration, it seems to be caused by the SST anomaly.

3.1.3 The wind field

The wind at 850 mb decreases and becomes more westerly in the regions with the largest precipitation increase. Also in these areas the wind converges in the lower layers, while it diverges at 200 mb (Fig. 5). Since it is coupled with ascending motion over the anomaly region we can conclude that the Hadley circulaton has been enhanced by the positive anomaly.

The wind field is reversed for the negative anomaly, but with less strength.

The wind field for the warm El-Nino anomaly compares quite well with the observed wind field deviation for October 1982. Even features in the vicinity of the anomaly are simulated; for example the outflow between 160°W and 100°W south of the equator and the inflow between 150°W and 150°E north of the equator. The change in the wind field is similar to the one obtained by Shukla and Wallace (1982).

3.1.4 The temperature field

The temperature field shows more structure than the other fields and will therefore be discussed in more detail:

a) The temperature deviation (Fig. 6) created by the warm anomaly clearly shows a warming in the anomaly region. This warming occurs in the lower layers, it is strongest over the eastern part of the Pacific and follows the

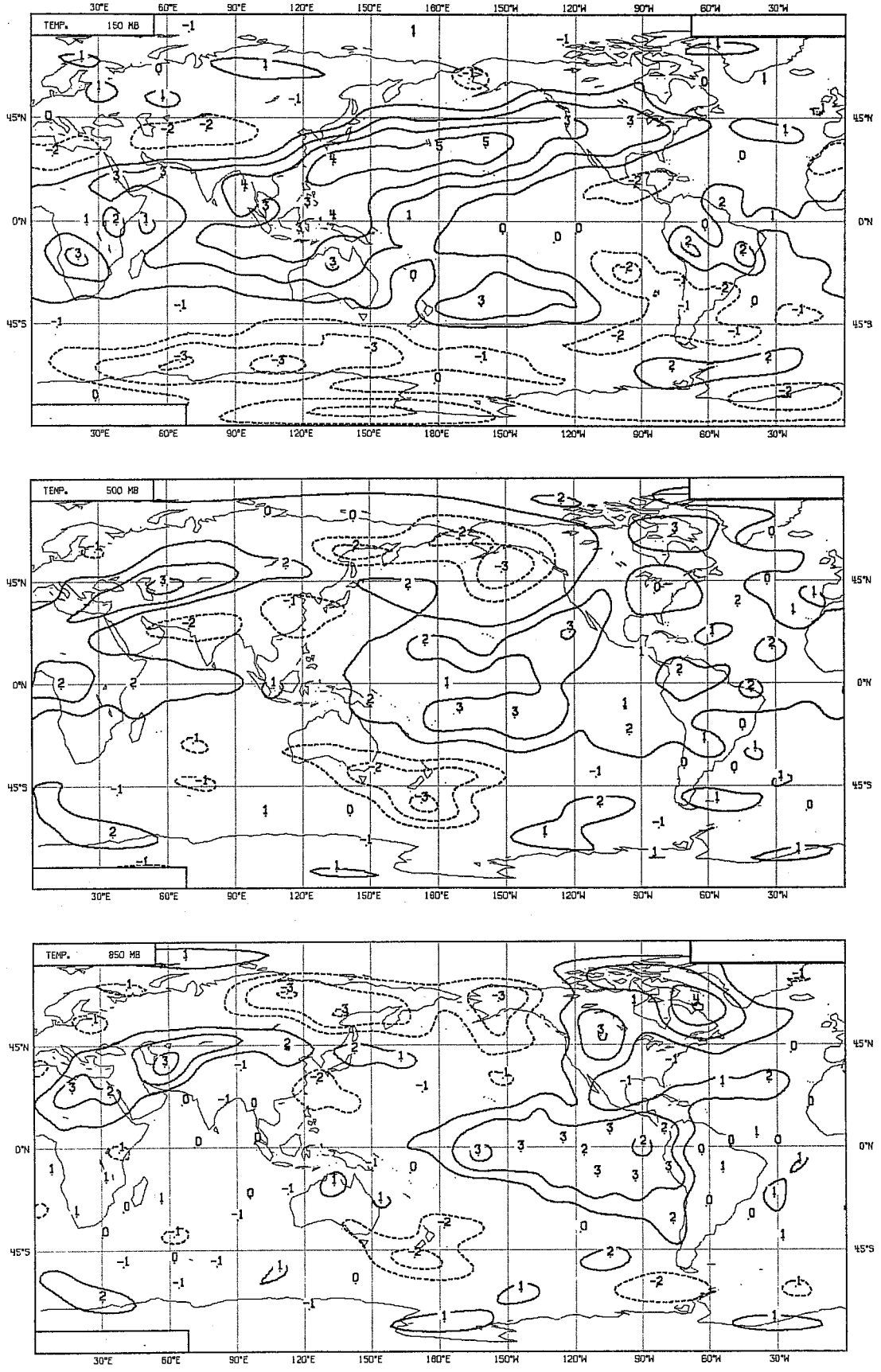

Fig. 6 The difference in the temperature field between the run with the positive anomaly and the control experiment. Top: 150 mb height, middle: 500 mb height, bottom: 850 mb height. (Contouringinterval $1^{o}C$).

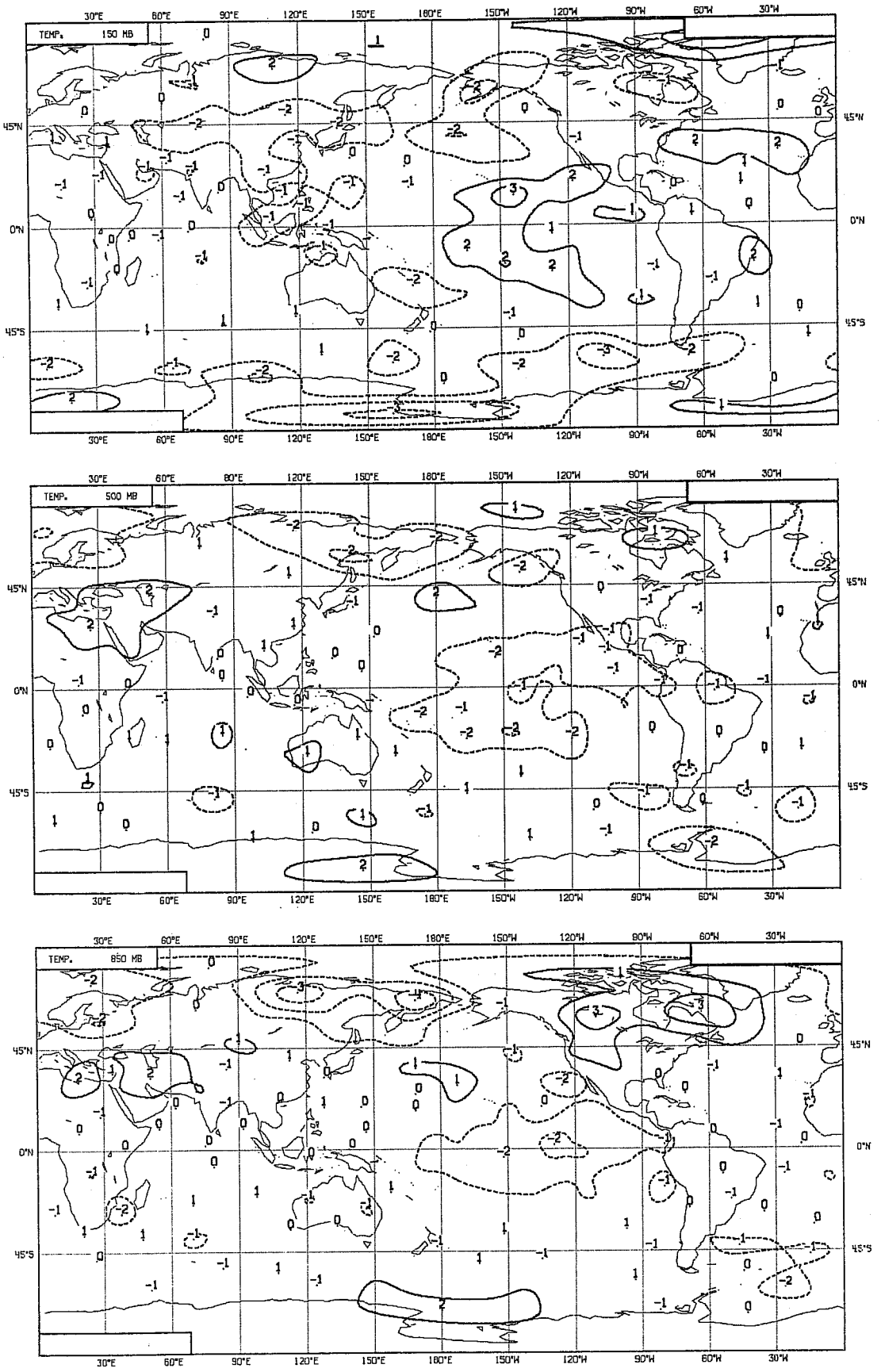

Fig. 7 The difference in the temperature field between the run with the negative anomaly and the control experiment. Top: 150 mb height, middle: 500 mb height, bottom: 850 mb height. (Contouring interval: $1^{o}C$).

shape of the anomaly. The warming extends further towards the poles at higher levels. Its maximum at 500 mb is not over the area where there is the largest precipitation increase, but in the subtropical high pressure belts in both hemispheres and west of the anomaly.

It seems that the release of latent heat by enhanced cumulus convection is counterbalanced by increased radiative and adiabatic cooling, so that the net effect in the tropics is small. The increased convection drives a more intense Hadley circulation whose increased sinking in the subtropical belt generates adiabatic warming.

b) The temperature deviation for the negative anomaly (Fig. 7) shows a cooling of the atmosphere up to 250 mb; in the lower layers this closely follows the shape of the anomaly. Above 250 mb a warming can be found, but the stratosphere remains unchanged. Less sensible heat flux into the lower layers of the atmosphere and decreased cumulus convection seem to be the prime cause of the cooling in the lower troposphere, while the warming in the higher troposphere seems to be generated by less radiative cooling (due to less clouds) and less adiabatic cooling (caused by less rising motion).

3.2 The response in the mid-latitudes

3.2.1 The height field

Fig. 8 shows the deviation of the 700 mb height field for the winter of year 9/10 of the model integration from the 10 year mean model winter. It shows positive pressure deviations over the Kamchatka peninsula and over Europe, separated by a negative one over Greenland.

The inclusion of the amomalies reverses this mean deviation in both cases, and the geographical distribution of the wavetrains generated by the anomalies seems to be independent of the sign of the anomaly.

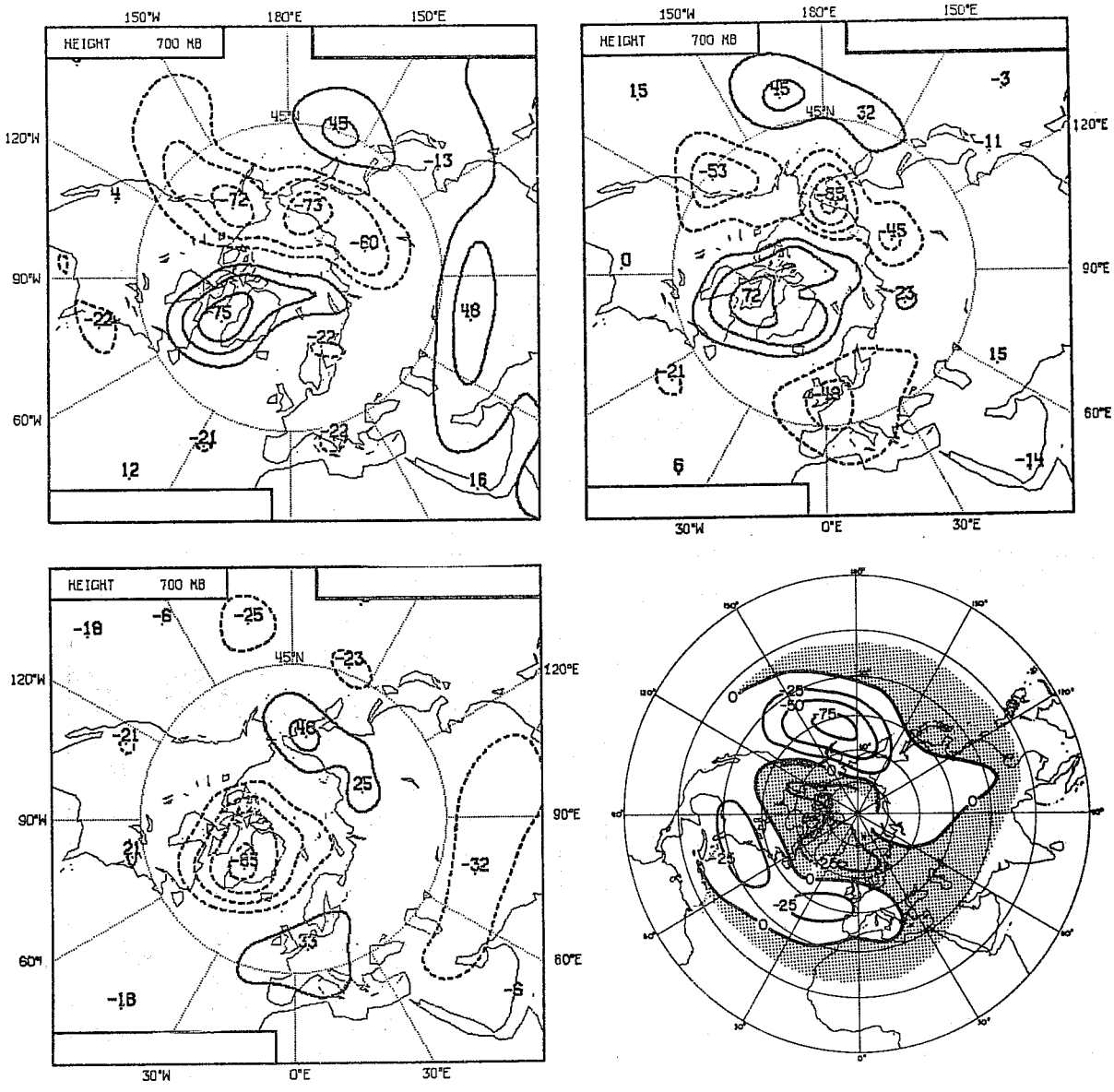

Fig. 8 The deviations created by the SST anomalies in the 700 mb height field for year 9/10. Top left: positive anomaly, top right: negative anomaly, bottom left: difference between control run and 10 year mean model climate, bottom right: observed correlation pattern (van Loon and Rogers, 1981). (Contouring interval: 20 m).

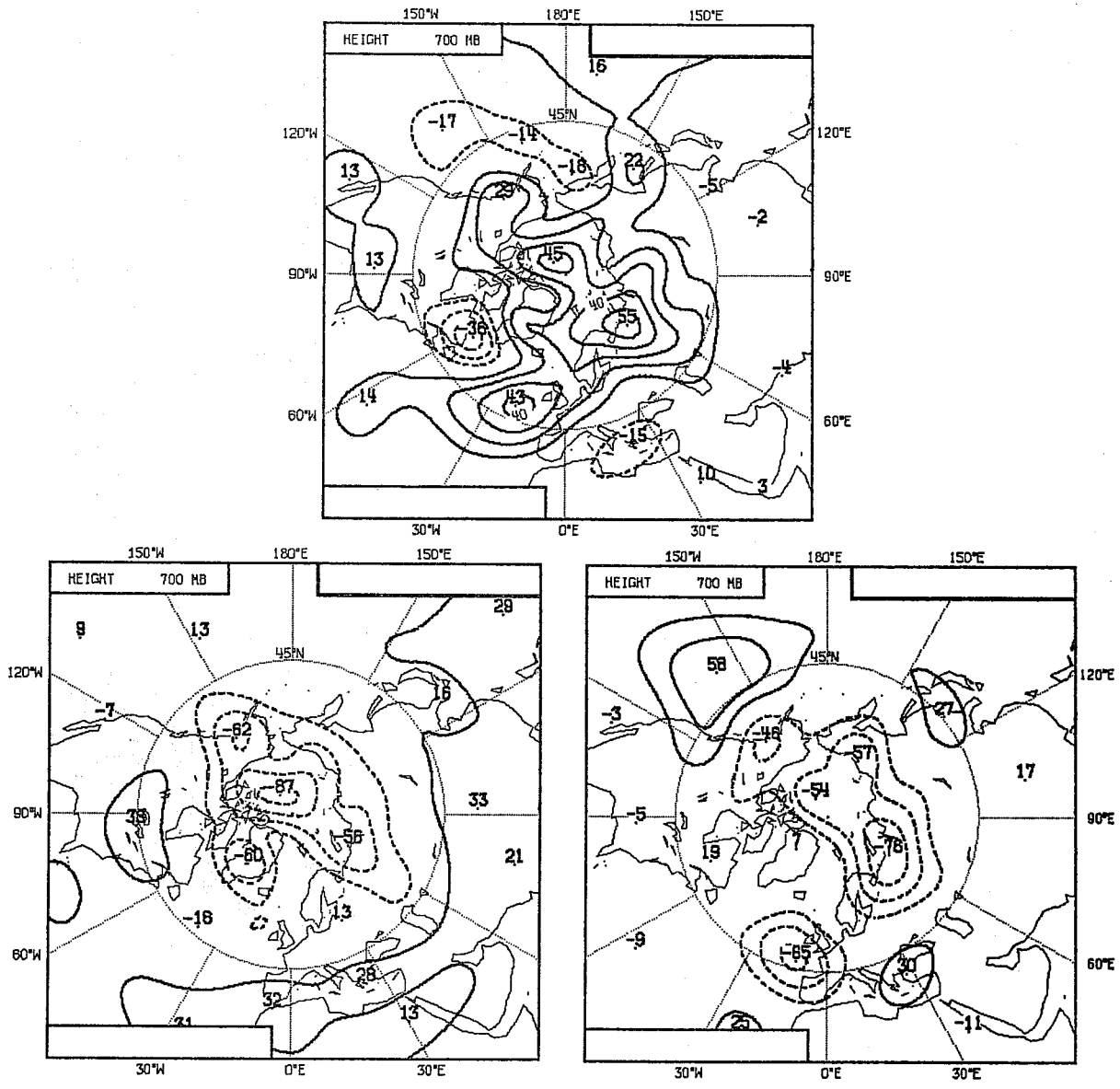

Fig. 9 The deviations created by the SST anomalies in the 700 mb height field for the year 1/2. Bottom left: positive anomaly, bottom right: negative anomaly, top: difference between control run and 10 year mean model climate: (contouring interval: 20 m).

Two different theories can be used to explain this phenomenon

a) following the ideas of Charney and DeVore (1979) one can assume that the atmosphere has discrete (basically two) stable states between which it oscillates. It can easily be brought from one stable state to the other by external forcing. It might be that in our experiment the implementation of the anomaly triggered the transition from one stable state to the other.

b) another explanation can be given if one consideres the change in the temperature field as described in section 3.1.4: since stationary perturbations generated by the anomalies can only travel in westerly currents (Charney and Drazin, 1961; Charney, 1969), one can assume that, in the case of the negative anomaly, the mid-latitude atmosphere only "sees" the warming in the higher layers. Its geographical position coincides with a warming in the experiment with the warm anomaly (in 500 mb). It can therefore trigger the same wavetrain.

When the positive and negative anomaly is applied to the first winter of the 10 year integration, the response in the mid-latitudes is again not directly correlated with the sign of the anomaly. In this experiment also, the anomalies reverse the deviation of the height field of year 1/2 compared to the model climate (Fig. 9). Since the height deviation of the model winter of year 1/2 (compared to the mean model climate) has the opposite sign to that of year 9/10 at the north pole, the anomalies in these two winters trigger wavetrains with opposite signs.

The minimum of the wavetrain simulated by the GCM in the ninth year over Alaska and Siberia, and the maximum of the wavetrain in the first year over the Pacific and Japan, can be identified as the Pacific/Siberia extremum of the observed correlation pattern (van Loon and Rogers,1981). The simulated extremum of the ninth year is shifted too far to the north and therefore falls partially onto the region with an opposite sign in the observed

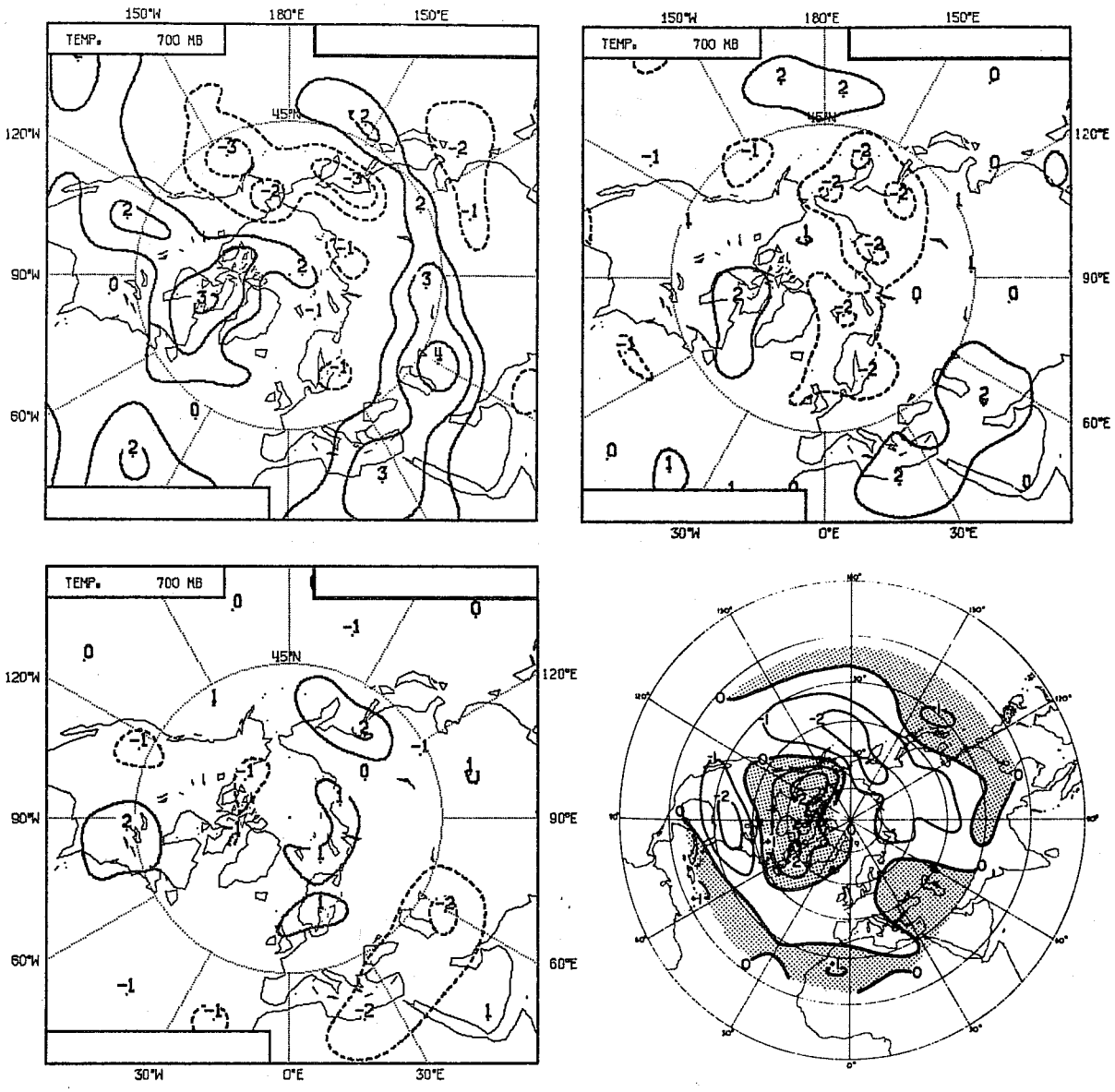

Fig. 10 The deviations created by the SST anomalies in the 700 mb temperature field. Top left: positive anomaly, top right: negative anomaly, bottom left: difference between control experiment and 10 year mean model climate, bottom right: observed correlation pattern (van Loon and Rogers, 1981). (Contouring interval: 1°C).

correlation. Over the Greenland/Newfoundland region, eastern North America and Europe the phases of the observed and simulated wavetrains agree quite well in the ninth winter. In the first winter simulation the polar part of the wavetrain is larger than observed and therefore shifts the European extremum further south. The fact that this correlation pattern can be found in the standard run as well as in the anomaly runs (with inversed sign), shows that this atmospheric phenomenon is also perceptible in the model atmosphere. This correlation pattern has also been found by Wallace and Gutzler (1981) in a recent study of teleconnections in the atmosphere.

In their numerical experiment Blackmon at al (1982) found a similar structure in the response pattern in their "twice warm" case. The fact that the height field deviation between the "cold" and the "warm" case is considerably weaker than the "twice warm" case also indicates a nonlinear response in their simulation. Their explanation of this phenomena was that the colder average temperature in the tropics reduces the capability of the air to retain moisture, which results in a decrease of 50% in the rainfall-deviation triggered by the anomaly. The response in the mid-latitudes should therefore only be half as large as in the "twice warm" experiment.

Shukla and Wallace (1982) started a number of 60 day integrations from observed data. As they stated, the shortness of their time series does not allow conclusions to be drawn about the response of the mid-latitudes, even though the tropical atmosphere responded as expected.

3.2.2 The temperature field

The mid-latitude temperature field of November to March at 700 mb for year 9/10 of the control run deviates only marginally from the model climate and shows no distinct wavetrain (Fig. 10). The negative anomaly creates a large cool area over Europe and northern Asia, while the positive anomaly cools the atmosphere in a belt from Alaska to China and warms it almost everywhere else in the northern hemisphere. In general, the pattern and strength of the

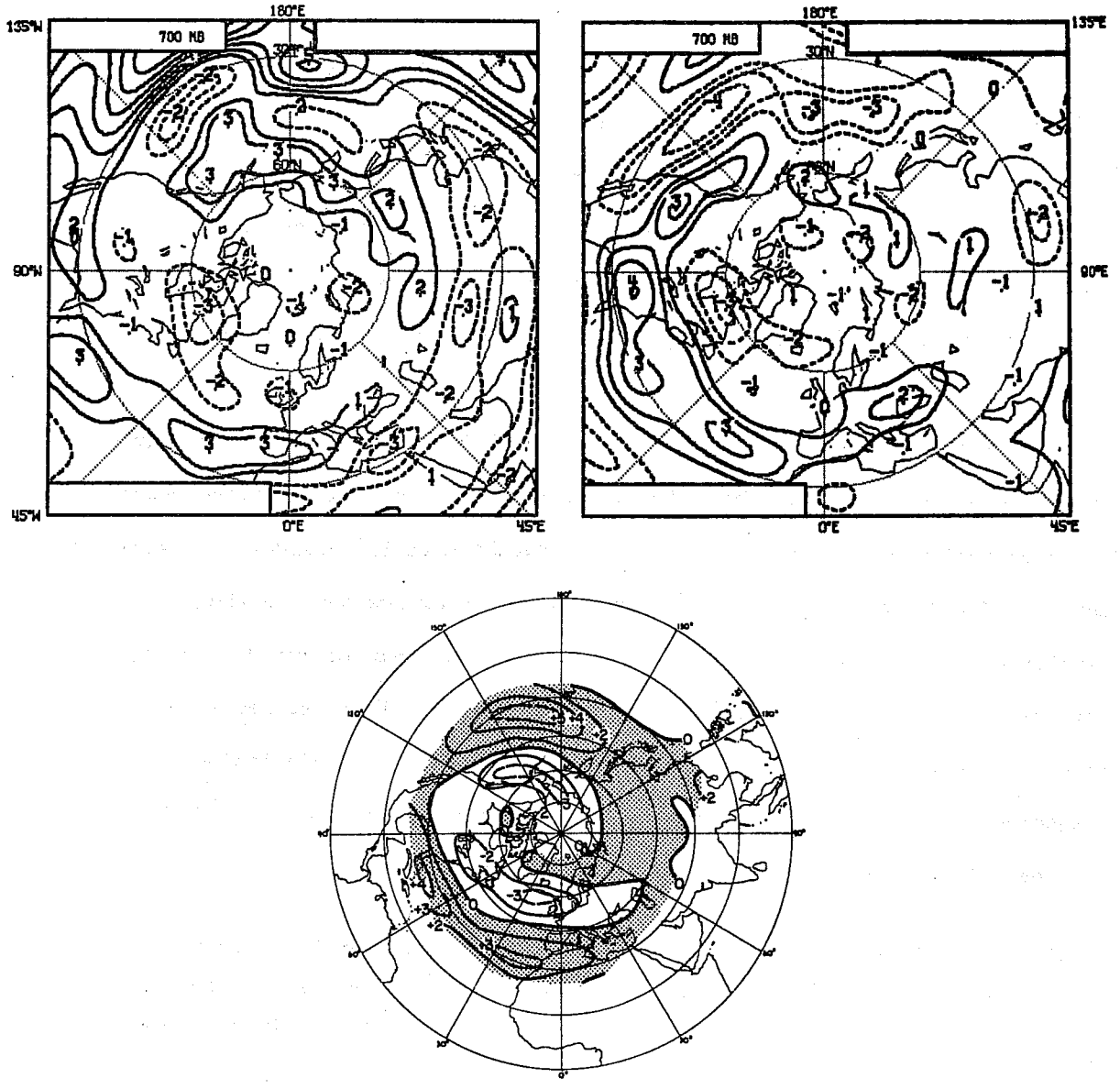

Fig. 11 The deviations created by the SST anomalies in the 700 mb zonal wind field. Top left: positive anomaly, top right: negative anomaly, bottom observed correlation pattern (van Loon and Rogers, 1981). (Contouring interval: 1 m/s).

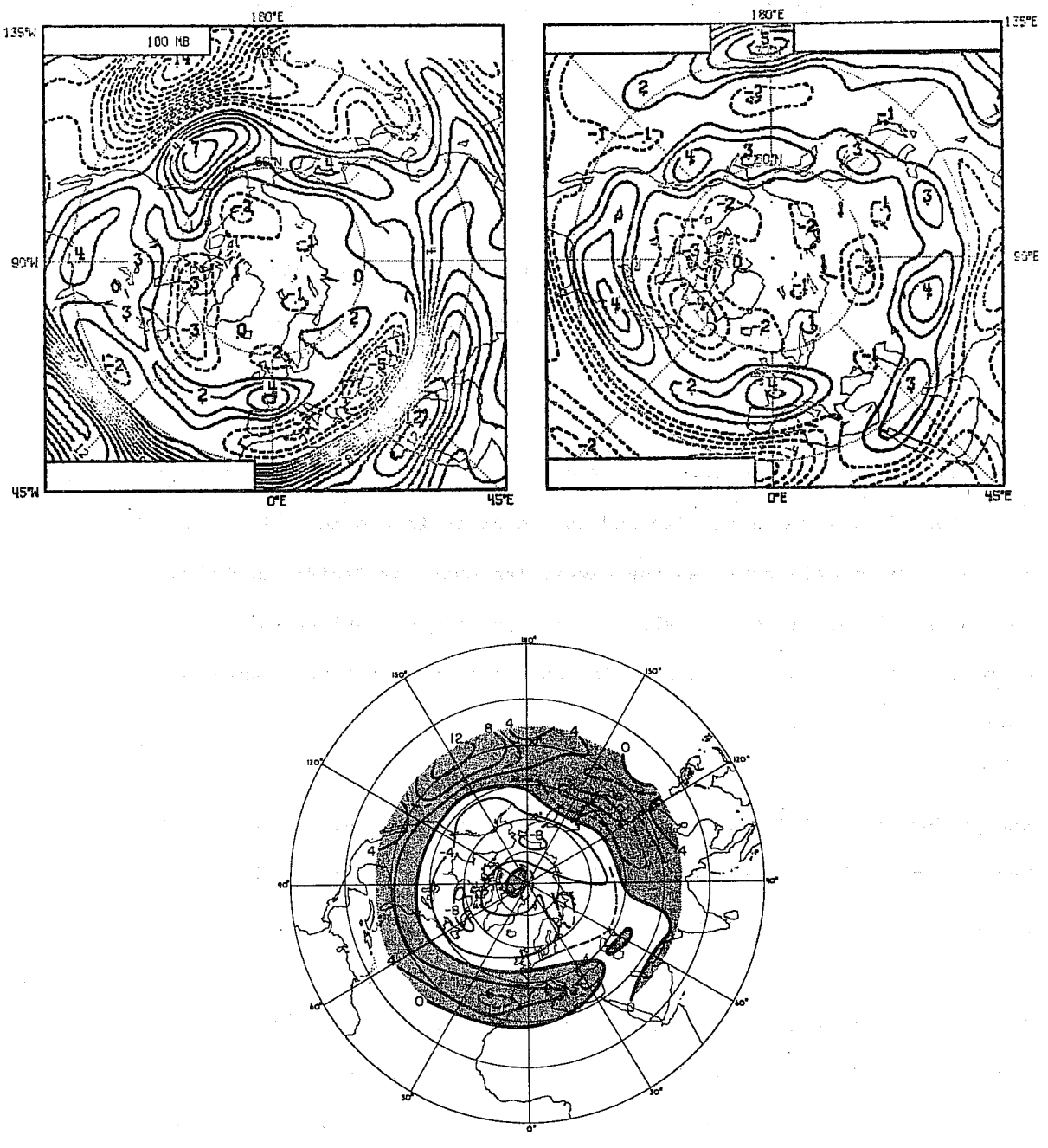

Fig. 12 The deviations created by the SST anomalies in the 100 mb zonal wind field. Top left: positive anomaly, top right: negative anomaly, bottom: observed correlation pattern (van Loon et al., 1982). (Contouring interval: 1 m/s).

simulated pattern agrees with the observed temperature deviations if one considers areas with small warming as areas with no or even negative temperature deviation. The area over the Pacific and China is not too well simulated.

3.2.3 The wind field

The mean zonal windfield of the control run (year 9/10) at 700 mb differs only over the Atlantic from the 10 year model climatology with values of at most 3 m/s (not shown).

The positive anomaly creates an increase of the westerly component almost everywhere in the north Pacific and in the Atlantic around 30°N (Fig. 11). The negative anomaly enhances the easterlies over the Pacific and also increases the westerlies as well over the subtropical Atlantic. Both anomalies create a weak easterly flow over the whole northern hemisphere north of about 50°N.

Except for the Pacific region between Alaska and Siberia, the agreement between the observed zonal wind deviation and the one simulated by the positive anomaly is quite good.

The observed correlation pattern in the lower stratosphere (van Loon et al, 1982) at 100 mb posesses a circumpolar structure; an area with positive values close to the North Pole is separated from a positive correlated area south of 40°N by a belt with negative correlation(Fig. 12). A similar structure can be found in the wind deviation generated by both anomalies, but the belts of equal deviation are shifted towards the North. Only in the tropics can a difference in the response be found which depends on the sign of the anomaly.

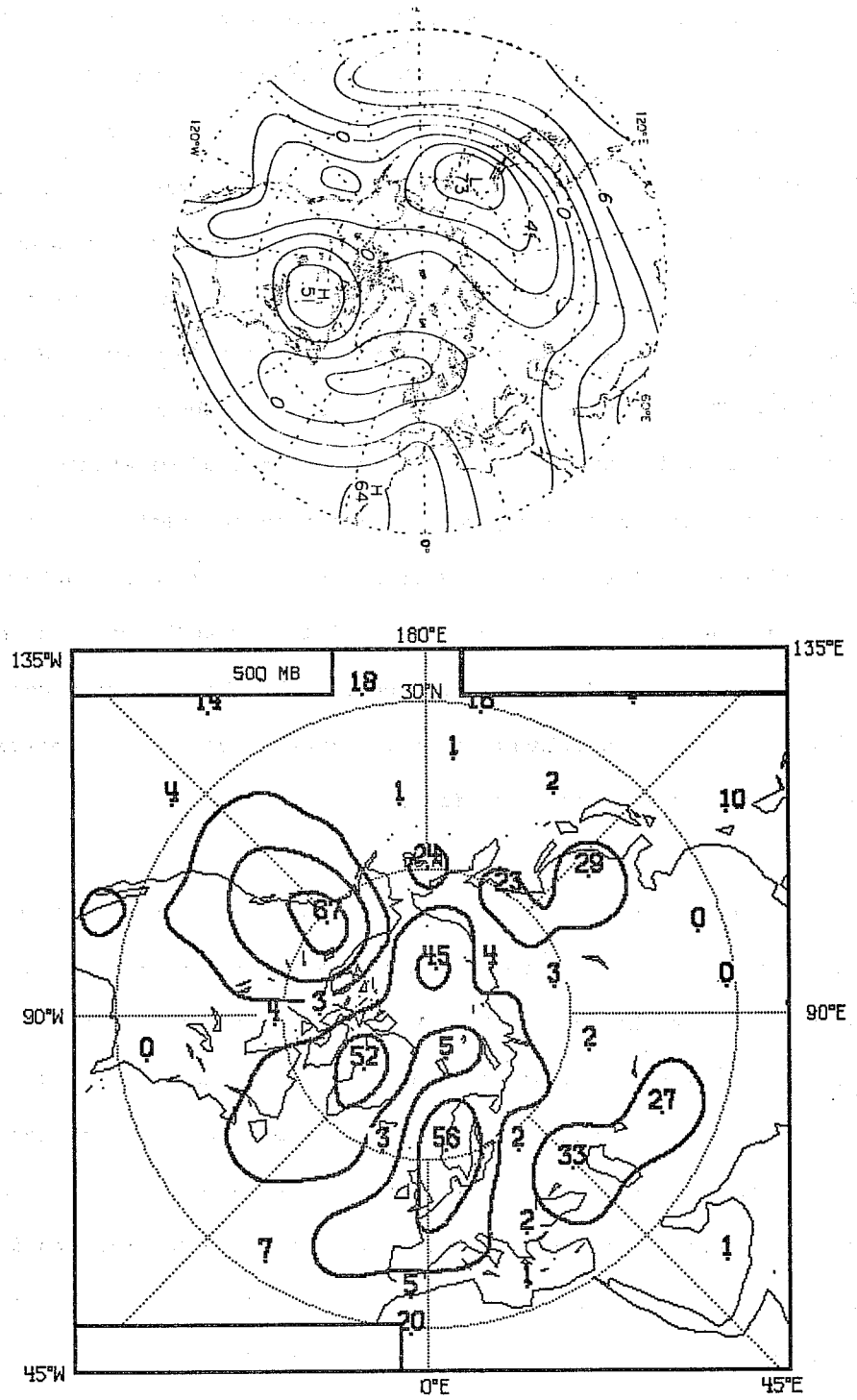

Fig. 13 The variance of the 500 mb response pattern for the positive anomaly (bottom: contouring interval 20 m, averaging period: 15 days) and the first EOF of the variance of the northern hemisphere winter (after Wallace and Gutzler, 1981).

3.3 Fluctuations in the response-pattern

The individual difference maps and even longer term means show a considerable variability in the response pattern. The mid-latitude variance of the height field difference can be found in Fig. 13. The variance also exhibits a wavetrain pattern whose extrema coincide with the extrema of the mean response. Its amplitude reaches about 75% of the mean deviation. This makes it clear that one has to use long time series to filter out a significant mean response pattern. The variance field can be compared with the first eigenvector of the observed variance of the north winter atmosphere (Wallace and Gutzler, 1981). This first eigenvector (it explains about 16% of the atmospheric variability) is similar to the "western Pacific" wavetrain, which, as Wallace and Gutzler suspect, has its roots in the central Pacific region. The similarity of the observed pattern with the simulated pattern might indicate that the SST anomalies are responsible for at least part of the atmospheric variability. This idea is supported by the fact that one also finds in the numerical experiments a large fluctuation in the tropical height and even precipitation deviation field.

The period of the fluctuations can be assessed by estimating the variance of low pass filtered time-series. It turns out that most of the variance is contained in waves longer than 30 days. Due to the shortness of the time-series it is impossible to give any exact value. An analysis of a time-series taken from single points in the central Pacific and over central north America indicates a period of 40-60 days. It seems possible that large scale tropical circulations, analogous to the ones observed and discussed by Madden and Julian (1971,1972), are generated or enhanced by the SST anomaly and excite oscillations in the mid-latitudes.

4. COMPARISON WITH SIMPLIFIED MODEL RESULTS

4.1 Tropical response

The tropical response of the height and wind field to a heating which is symmetric about the equator has been analysed by Gill (1980) and by Heckley

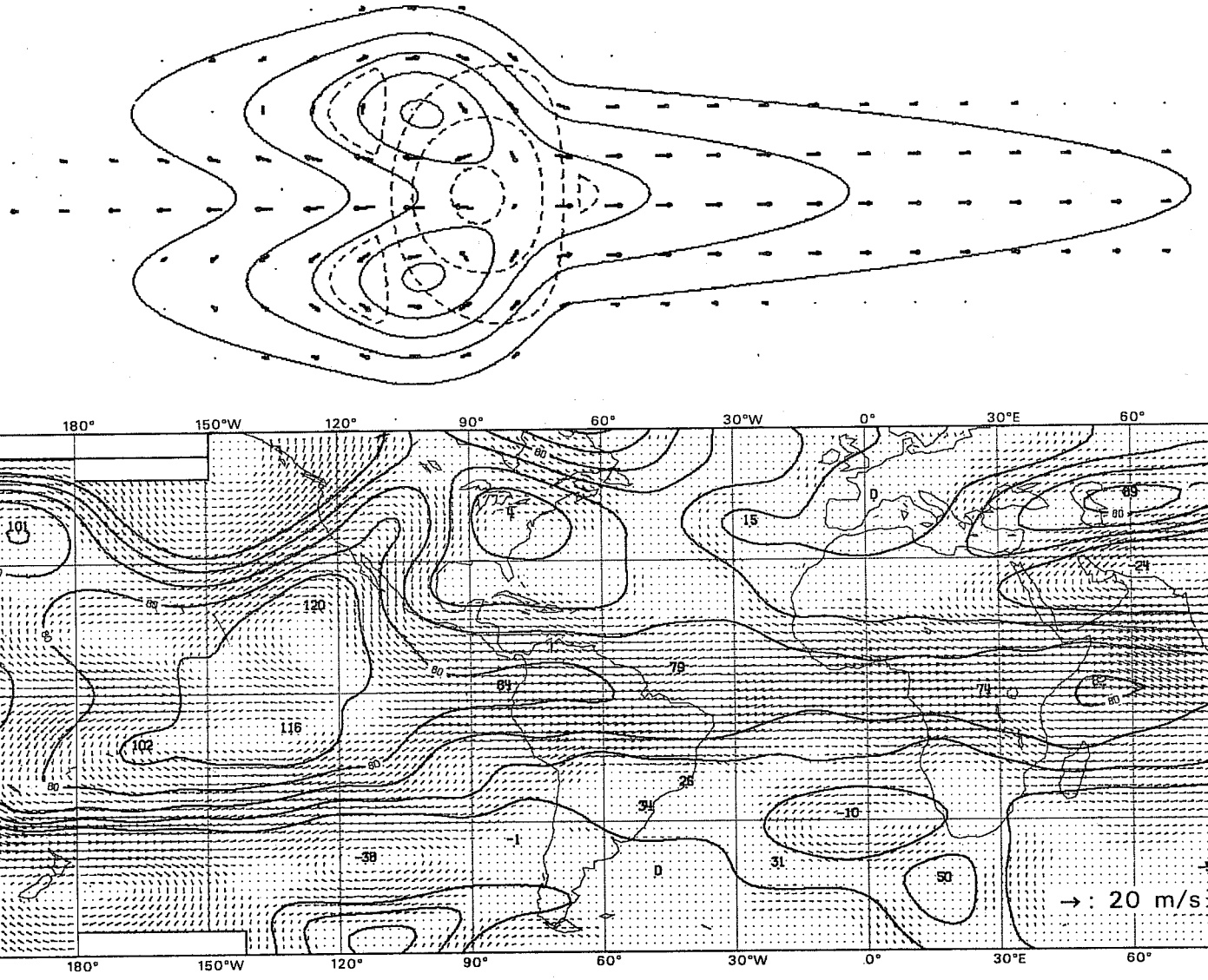

Fig. 14 The difference in the wind and height field between the run with the positive anomaly and the control experiment (bottom) in 200 mb height (negative contours have been supressed), and the flow anomaly simulated by a shallow water equation model (top) for a heating at the equator (Heckley and Gill 1983).

and Gill (1983) using a shallow water equation model. They found that after an initial adjustment period of about 30 days, a steady planetary wave develops around the heat source (Fig.14). This wave has a space-ship like shape with ascent over the heatsource and descent and outflow in the surrounding area (in the upper troposphere). The height field deviation shows an indentation west of the source region along the equator and a tail east of it.

In the GCM experiments, the height and the wind field at 200 mb clearly bear some resemblance to the results of the simplified model. The areas of ascent appear twice (one at 160°W, the other at 130°W), and they are connected with two areas of maximum precipitation increase.

The tail which is east of the heat source can also be found, but it is not clear whether it only reaches the African coast or goes around the whole globe as far as Borneo.

The northern and southern flank of the pressure deviation do not have quite the same shape as found in the idealized case. This might be caused by the double cell structure of the heat source or by the neglect of a basic state zonal flow in the idealized model, but interaction with mid-latitude disturbances cannot be excluded. The GCM experiment with the negative anomaly follows fairly closely the results obtained with the simplified model.

It appears, therefore, that the response of the tropical atmosphere to mid-atmospheric heating can, to a first approximation, be described by a linear model. However, this mid-atmospheric heating, created by the enhanced latent heat release and triggered by the SST anomaly cannot be simulated with the linear model due to the non-linear dependence of the saturation mixing ratio on the temperature.

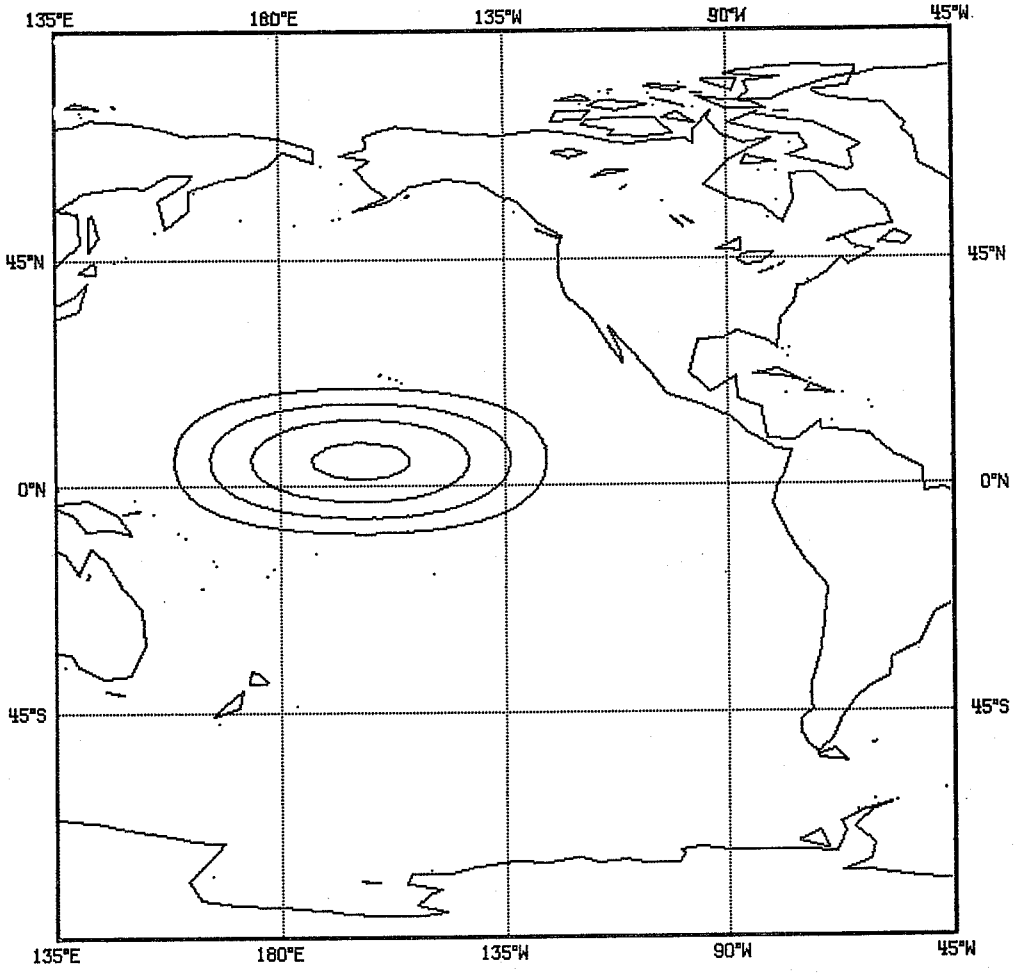

Fig. 15 The geographical position of the heatsource for the linear and barotropic model.

4.2 Mid-latitude results

Two simplified model experiments have been launched to investigate the response of the mid-latitudes to the El-Nino anomaly.

The first integration was performed with the linear baroclinic model as described by Simmons (1982). In this model the zonally averaged flow for the January climate is perturbed by an elliptical heat source situated in the region of the El-Nino anomaly (Fig. 15). The maximum heating was assumed to be 5 K/day at 400 mb. The response pattern showed little sensitivity to the vertical distribution of the heat source.

Since the GCM experiments with the negative and positive anomalies showed a warming in the higher troposphere, this simulation with the linear model can perhaps be assumed to be relevant for both model runs.

The response pattern of the linear model (Fig. 16) displays a a positive pressure deviation over the anomaly region which goes over into a negative deviation over North America and the north Pacific. Here it continues with an increased height field over the polar region of the American continent and Europe separated by a low pressure belt north of Scandinavia.

In its shape and number of extrema, this wavetrain compares quite well with the GCM simulations, but over Europe it is out of phase and its wavelength appears to be smaller.

The other test used the barotropic model with zonally-variing basic state described by Simmons (1982) and Simmons et al (1983). In this model the average flow from November to March of year 9/10 of the 10 year integration has been perturbed by a vorticity forcing which simulates the effect of a heat source. The geographical position of this vorticity forcing is equivalent to the heatsource in the experiment with the linear baroclinic model. The barotropic model has been integrated until the response pattern became steady (in this case 30 days).

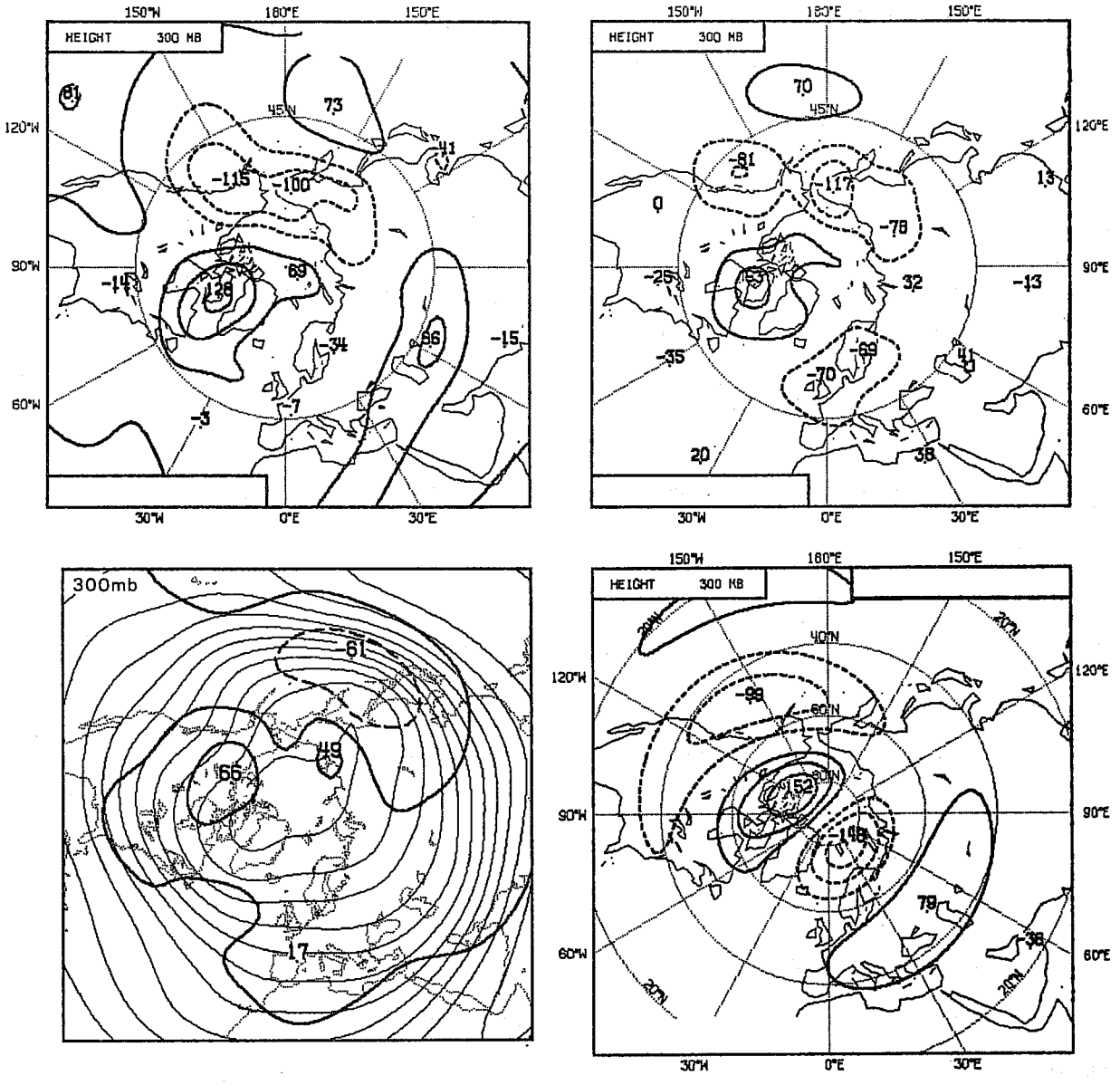

Fig. 16 The response of the 300 mb height field to an anomaly. Top left: GCM, positive anomaly, top right: GCM, negative anomaly, bottom right: linear model, bottom left: barotropic model.

The response pattern of the barotropic model does not show a well defined wave train. However, there is a region of lower pressure which stretches from China, over the north Pacific and Mexico, and continues as far as Mauretania. This pressure deviation can also be found in the GCM experiment with the positive anomaly.

The rest of the northern hemisphere shows an increase in the pressure which is not found in any other model run. The maximum of this positive pressure deviation, however, almost coincides with the positive response over Newfoundland in the other experiments.

Even though it appears as if the response to the anomaly can be represented quite well with the linear model, it has to be mentioned that the effect of the negative anomaly can not be simulated by simply inserting a cooling in the linear model. In the atmosphere ,due to nonlinear effects, even a cold anomaly creates a heating at the appropriate heights. On the other hand, the geographical position of the wavetrains seem to be rather insensitive to the height at which the heating is situated; therefore in the linear model one can use a positive heating even for a negative anomaly.

5. SUMMARY AND CONCLUSIONS

The experiments reported here have shown that in the tropics the model atmosphere responds linearly and that the response can be simulated by a simple model. However, the connection between a SST nomaly and the resulting mid-atmospheric heating is non-linear.

The SST anomaly influences the state of the southern oscillation. A positive SST anomaly leads to a lower than average surface pressure in the central Pacific, whereas a negative anomaly leads to a higher one.

The heating seems not only to occur at the location of the largest precipitation increase, but also (due to adiabatic warming in the area of sinking motion) in the subtropical part of the Hadley circulation.

The mid-latitudes show a response pattern which resembles the observed correlation pattern. Slight shifts in the phase might be attributed to a number of known deficiencies in the ECMWF model, like the tendency to move depressions too far towards the poles and too far inland (Arpe,1983). The mid-latitude response is not unequivocally related to the sign of the anomaly and therefore can only be explained by linear theories with difficulty. The coupling mechanism between mid-latitudes and tropics seems to be highly non-linear and demands further investigations. It is interesting to note that GCM sensitivity experiments performed by other groups indicate a similar behaviour in the mid-latitudes as found this study.

Superimposed on the mid-latitudinal wavetrain are low frequency fluctuations (periods of more than 15 days) whose amplitude is similar to the size of the total response. Therefore, when different averaging periods are used, the mean wavetrain appears to move with time. The cause of the fluctuations, which can also be found in the precipitation, is not known. However it is possible that they might be generated by a similar mechanism to that described by Madden and Julian (1971,1972), in which a fluctuating heat source triggers migrating wavetrains.

A comparison of the recent (1982/1983) El-Nino event with the model simulations indicates that dynamical feedbacks from the atmosphere to the ocean influence the atmosphere on a time-scale of a month, and should therefore not be neglected in a long integration.

ACKNOWLEDGEMENTS

The author wishes to express thanks to his colleagues at ECMWF, specially Dr.Tiedtke, Dr.Simmons and Dr.Heckley, who made numerous suggestions in discussions of the experiments. The study could not have been carried out without the enthusiastic support of Dr.Bengtsson (ECMWF), Prof.Hasselmann (MPI Hamburg) and Prof.G.Fischer (Universität Hamburg). Part of the computer time was made available from the "Deutscher Wetterdienst" (FRG) and the "Meteorlogié Nationale" (France).

REFERENCES

Arpe, K.,1983: Diagnostic evaluation of analysis and forecast climate of the ECMWF model; Proceedings to the ECMWF seminar on "Interpretation of numerical weather prediction products", 99-140

Baede, A., M. Jarraud and U. Cubasch, 1979: Adiabatic formulation and organisation of ECMWF's spectral model. ECMWF Tech.Rep.No.15, 40 pp.

Berlage, H.P.,1957: Fluctuations of the general circulation of more than one year, their nature and their prognostic value; Medelingen en Verhandelingen, No. 69, Koninklijk Nederlands Meteorologisch Instituut, 152pp.

Bjerknes, J.,1966: A possible response of the atmospheric Hadley circulation to the equatorial anomalies of the ocean surface temperature. Tellus, 18, 820-829.

Bjerknes, J., 1969: Atmospheric teleconnections from the equatorial Pacific. Mon.Wea.Rev., 97, 163-172.

Blackmon, M.L., J.E. Geisler and E.J. Pitcher, 1982: A general ciculation model study of January climate anomaly patterns associated with interannual variation of equatorial Pacific SST's. Proceedings to the WGNE workshop on SST sensitivity experiments held in Princeton, December 1982.

CAC 1, Special Climate Diagnostic Bulletin, 10.11.1982: A major warm episode in the eastern equatorial Pacific ocean. Climate Analysis Centre, NOAA National Weather Service, Washington.

CAC 2, Special Climate Diagnostic Bulletin, 14.02.1983: The equatorial pacific warm episode reaches its mature state. Climate Analysis Centre, NOAA National Weather Service, Washington.

CAC 3, Special Climate Diagnostic Bulletin, 15.04.1983: Update on the 1982-83 equatorial Pacific warm episode. Climate Analysis Centre, NOAA National Weather Service, Washington.

Charney, J.G., 1969: A further note on large-scale motions in the Tropics. J.Atmos.Sci., 20, 607-609.

Charney, J.G. and P.G. Drazin, 1961: Propagation of planetary-scale disturbances from the lower into the upper atmosphere. J.Geophys.Res., 74, 83-109.

Charney, J.G. and J.G. DeVore, 1979: Multiple flow equilibria in the atmosphere and blocking. J.Atmos.Sci., 36, 1205-1216.

Chervin, R.M., W.M. Washington and S.H. Schneider, 1976: Testing the significance of the response of the NCAR general circulation model to north Pacific ocean surface temperature anomalies. J.Atmos.Sci., 33, 413-423.

Gill, A.E., 1980: Some simple solutions for heat induced tropical circulation; Quart. J.Roy.Met.Soc., 106, 447-462.

Heckley, W.A. and A.E. Gill, 1983: Some simple analytical solutions to the problem of forced equatorial long waves. submitted to Quart.J.Roy.Met.Soc.

Horel, J.D. and M.J. Wallace, 1981: Planetary scale atmospheric phenomena associated with the interannual variability of sea-surface temperature in the equatorial Pacific. Mon.Wea.Rev., 109, 813-829.

Hoskins, B. and D. Karoly, 1981: The steady linear response of a atmosphere to thermal and orographic forcing. J.Atmos.Sci., 38, 1179-1196.

Houghton, D.D., J.E. Kutzbach, M. McClintock and D. Suchman, 1974: Response of a general circulation model to sea temperature perturbations. J.Atmos.Sci., 31, 856-868.

Huang, J.C.K., 1978: Response of the NCAR general circulation model to north Pacific sea-surface-temperature anomalies. J.Atmos.Sci., 35, 1164-1179.

Kutzbach, J.E., R.M.Chervin and D.D. Houghton, 1977: Response of the NCAR general circulation model to prescribed changes in the ocean surface temperatures. Part I.: Mid-latitudinal changes. J.Atmos.Sci., 34, 1200-1213.

Lau, N.C., 1981: A diagnostic study of recurrent meteorological anomalies appearing in a 15 year simulation with the GFDL general circulation model. Mon.Wea.Rev., 109, 2287-2286.

Madden, R.A., and P.R. Julian, 1972: Description of global-scale cells in the tropics with a 40-50 day period. J.Atmos.Sci., 29, 1109-1123.

Manabe, S. and D.G. Hahn, 1981: Simulation of atmospheric variability. Mon.Wea.Rev., 109, 2260-2286.

Namias, J., 1969: Seasonal interactions between the north Pacific ocean and the atmosphere during the 1960's. Mon.Wea.Rev., 97, 173-192.

Rasmusson, E. and T. Carpenter, 1982: Variations in the tropical sea-surface-temperature and surface wind fields associated with the Southern Oscillation/El Nino. Mon.Wea.Rev., 110, 254.284.

Rilat, M.F. and M.A. Thepaut, 1982: Analyse du un cycle hydrologique dans un experience de dix ans de simulation du climat. Note de Travail de l'Ecole Nationale de la Meteorologie No.20, Meteorologie Nationale, 77 rue des Sevres, Boulogne, France.

Rowntree, P.R., 1972: The influence of tropical east Pacific ocean temperatures on the atmosphere. Quart.J.Roy.Met.Soc., 98, 290-321.

Simmons, A.J., 1982: The forcing of stationary wave motion by tropical diabatic forcing: Quart.J.Roy.Met.Soc., 198, 507-534.

Simmons, A.J., M.J. Wallace and G.W. Branstator, 1982: Barotropic wave propagation and instability, and atmospheric teleconnection patterns. J.Atm.Sci., in press.

Shukla, J. and J. M. Wallace, 1982: Numerical simulation of the atmospheric response to equatorial Pacific SST anomalies. Proceedings to the WGNE workshop on SST sensitivity experiments held in Princeton, N.J., USA, December 1982.

Tiedtke, M., J.F. Geleyn, A. Hollingsworth, J.F. Louis, 1978: ECMWF-model parametrisation of subgrid processes. ECMWF Tech.Rep.No.10, 46pp.

van Loon, H. and P.A. Madden, 1981: The southern Oscillation. Part I: Global associations with Pressure and Temperature in northern winter. Mon.Wea.Rev., 109, 1150-1162.

van Loon, H., and J.C.Rogers, 1981: The southern oscillation troposphere in the northern winter. Mon.Wea.Rev., 109, 1163-1168.

van Loon, H., C.S. Cerefos, and C.C. Repapis, 1982: The southern oscillation in the stratosphere; Mon.Wea.Rev., 110, 225-229.

Volmer, J.P., M. Deque and D. Rousselet, 1983: Long range behaviour of the atmosphere: A comparison between simulation and reality. Meteorologie Nationale, 77 rue des Sevres, 92100 Boulogne, France.

Wallace, J.M., and D.S. Gutzler, 1981: Teleconnections in the geopotential height field during the northern hemisphere winter; Mon.Wea.Rev., 109, 784-812.

Webster, P.J., 1981: Mechanisms determining the atmospheric response to sea-surface temperature anomalies. J.Atmos.Sci., 38, 554-571.

ECMWF PUBLISHED TECHNICAL REPORTS

No. 1 A Case Study of a Ten Day Prediction

No. 2 The Effect of Arithmetic Precisions on some Meteorological Integrations

No. 3 Mixed-Radix Fast Fourier Transforms without Reordering

No. 4 A Model for Medium-Range Weather Forecasting - Adiabatic Formulation

No. 5 A Study of some Parameterizations of Sub-Grid Processes in a Baroclinic Wave in a Two-Dimensional Model

No. 6 The ECMWF Analysis and Data Assimilation Scheme - Analysis of Mass and Wind Fields

No. 7 A Ten Day High Resolution Non-Adiabatic Spectral Integration: A Comparative Study

No. 8 On the Asymptotic Behaviour of Simple Stochastic-Dynamic Systems

No. 9 On Balance Requirements as Initial Conditions

No.10 ECMWF Model - Parameterization of Sub-Grid Processes

No.11 Normal Mode Initialization for a multi-level Gridpoint Model

No.12 Data Assimilation Experiments

No.13 Comparison of Medium Range Forecasts made with two Parameterization Schemes

No.14 On Initial Conditions for Non-Hydrostatic Models

No.15 Adiabatic Formulation and Organization of ECMWF's Spectral Model

No.16 Model Studies of a Developing Boundary Layer over the Ocean

No.17 The Response of a Global Barotropic Model to Forcing by Large-Scale Orography

No.18 Confidence Limits for Verification and Energetics Studies

No.19 A Low Order Barotropic Model on the Sphere with the Orographic and Newtonian Forcing

No.20 A Review of the Normal Mode Initialization Method

No.21 The Adjoint Equation Technique Applied to Meteorological Problems

No.22 The Use of Empirical Methods for Mesoscale Pressure Forecasts

No.23 Comparison of Medium Range Forecasts made with Models using Spectral or Finite Difference Techniques in the Horizontal

No.24 On the Average Errors of an Ensemble of Forecasts

No.25 On the Atmospheric Factors Affecting the Levantine Sea

No.26 Tropical Influences on Stationary Wave Motion in Middle and High Latitudes

ECMWF PUBLISHED TECHNICAL REPORTS

No.27 The Energy Budgets in North America, North Atlantic and Europe Based on ECMWF Analyses and Forecasts

No.28 An Energy and Angular-Momentum Conserving Vertical Finite-Difference Scheme, Hybrid Coordinates, and Medium-Range Weather Prediction

No.29 Orographic Influences on Mediterranean Lee Cyclogenesis and European Blocking in a Global Numerical Model

No.30 Review and Re-assessment of ECNET - a private network with Open Architecture

No.31 An Investigation of the Impact at Middle and High Latitudes of Tropical Forecast Errors

No.32 Short and Medium Range Forecast Differences Between a Spectral and Grid Point Model. An Extensive Quasi-Operational Comparison

No.33 Numerical Simulations of a Case of Blocking: The Effects of Orography and Land-Sea Contrast

No.34 The Impact of Cloud Track Wind Data on Global Analyses and Medium Range Forecasts

No.35 Energy Budget Calculations at ECMWF: Part I: Analyses

No.36 Operational Verification of ECMWF Forecast Fields and Results for 1980-1981

No.37 High Resolution Experiments with the ECMWF Model: A Case Study

No.38 The Response of the ECMWF Global Model to the El-Nino Anomaly in Extended Range Prediction Experiments